Plant Physiology®

BELL1 interacts with *CRABS CLAW* and *INNER NO OUTER* to regulate ovule and seed development in pomegranate

Yujie Zhao [iD],[1,2] Yuying Wang [iD],[1,2] Ming Yan [iD],[1,2] Cuiyu Liu [iD][1,2] and Zhaohe Yuan [iD][1,2,*]

1 Co-Innovation Center for Sustainable Forestry in Southern China, Nanjing Forestry University, Nanjing 210037, China
2 College of Forestry, Nanjing Forestry University, Nanjing 210037, China

*Author for correspondence: zhyuan88@hotmail.com (Z.Y.)
The author responsible for distribution of materials integral to the findings presented in this article in accordance with the policy described in the Instructions for Authors (https://academic.oup.com/plphys/pages/General-Instructions) is Zhaohe Yuan (zhyuan88@hotmail.com).

Abstract

Pomegranate (*Punica granatum*) flowers are classified as bisexual flowers and functional male flowers. Functional male flowers have sterile pistils that show abnormal ovule development. In previous studies, we identified *INNER NO OUTER* (*INO*), *CRABS CLAW* (*CRC*), and *BELL1* (*BEL1*), which were specifically expressed in bisexual and functional male flowers. However, the functions of ovule identity genes and the mechanism underlying ovule sterility in pomegranate remain unknown. Here, we found that the integument primordia formed and then ceased developing in the ovules of functional male flowers with a vertical diameter of 8.1–13.0 mm. Megaspore mother cells were observed in bisexual flowers when the vertical diameters of flowers were 10.1–13.0 mm, but not in functional male flowers. We analyzed the expression patterns of ovule-related genes in pomegranate ovule sterility and found that *PgCRC* mRNA was highly expressed at a critical stage of ovule development in bisexual flowers. Ectopic expression of *PgCRC* and *PgINO* was sufficient to increase seed number in transgenic lines. *PgCRC* partially complemented the Arabidopsis (*Arabidopsis thaliana*) *crc* mutant, and *PgINO* successfully rescued the seeds set in the Arabidopsis *ino* mutant. The results of yeast two-hybrid assays, bimolecular fluorescence complementation assays, and genetic data analyses showed that PgCRC and PgINO directly interact with PgBEL1. Our results also showed that PgCRC and PgINO could not interact directly with MADS-box proteins and that PgBEL1 interacted with SEPALLATA proteins. We report the function of PgCRC and PgINO in ovule and seed development and show that PgCRC and PgINO interact with PgBEL1. Thus, our results provide understanding of the genetic regulatory networks underlying ovule development in pomegranate.

Introduction

Ovules are the female reproductive organs of angiosperms and the progenitors of seeds. Ovule initiation in plants determines the maximum ovule number and substantially affects the seed number of the fruit. In Arabidopsis (*Arabidopsis thaliana*), ovule primordia arise from the placenta within the gynoecium (Schneitz et al., 1995). Following the elongation of the finger-like ovule primordia, the inner integument

initiates as a ring around the upper half of the chalaza region. Below the inner integument primordia, the outer integument initiates on the side of the ovule oriented toward the base of the carpel (Gasser and Skinner, 2019). The outer integument grows asymmetrically by increasing cell divisions on the side facing the central septum, resulting in a curved ovule (Robinson-Beers et al., 1992; Schneitz et al., 1995). Genetic and molecular analyses have identified several genes

Open Access

that are involved in ovule identity determination and development. *AINTEGUMENTA* (*ANT*), *NOOZLE* (*NZZ*), and *CRABS CLAW* (*CRC*) have been reported to play vital roles in ovule primordia initiation (Battaglia et al., 2009), and integument initiation is controlled by *ANT* and *WUSCHEL* (*WUS*). Moreover, *INNER NO OUTER* (*INO*), *PHABULOSA* (*PHB*), and *ABERRANT TESTA SHAPE* (*ATS*) play important roles in determining inner and outer integument development (Battaglia et al., 2009).

CRC is a YABBY transcription factor that acts as a transcriptional activator in nectary development and carpel fusion, and is also involved in floral meristem termination via transcriptional repression (Gross et al., 2018; Castañeda et al., 2022). Previous studies have reported that the carpels of *crc* mutants are broader, shorter, and contain fewer ovules than those of the wild-type (WT), suggesting that *CRC* is involved in ovule primordia initiation (Alvarez and Smyth, 1999; Bowman and Smyth, 1999; Alvarez and Smyth, 2002). *CRC* and *INO*, in combination with *KANADI* (*KAN*) and *ETTIN* (*ETT*), regulate the adaxial–abaxial patterning of carpels (Lora et al., 2015; Sablowski, 2015). The transient overexpression of *PeDL1*, which is a gene homologous to *DROOPING LEAF/CRABS CLAW* (*DL/CRC*) in orchids (*Phalaenopsis equestris*), causes abnormal development of ovules (Chen et al., 2021). Recent studies have also shown that *CRC* is required for ovule differentiation and development (Chen et al., 2021; Gong et al., 2021).

INO belongs to the YABBY family and is essential for ovule development in plants (Baker et al., 1997; Villanueva et al., 1999), such that the ovules of *ino* mutants lack the outer integument (Balasubramanian and Schneitz, 2002). *INO* is specifically expressed on one side of the central region of each ovule primordium in the cells that give rise to the outer integument. During ovule development in Arabidopsis, the growth of the outer integument is restricted primarily to the side of the ovule facing the basal region of the gynoecium. This asymmetry is mediated via *SUPERMAN* (*SUP*), which restricts *INO* expression to the basal side of the gynoecium in developing ovules (Meister et al., 2002). *CRC* can substitute for *INO* in the promotion of integument growth, but does not respond to *SUP* regulation (Gallagher and Gasser, 2008). *VviINO*, a gene homologous to *INO* in grapevine (*Vitis vinifera*), partially complements the asymmetric growth of the outer integument in Arabidopsis *ino* mutants (di Rienzo et al., 2021).

Pomegranate (*Punica granatum* L.) trees produce large numbers of bisexual flowers (that produce fruits) and functional male flowers (that typically drop and fail to set fruit; Wetzstein et al., 2011). Bisexual flowers have numerous anatropous ovules. In contrast, the ovules in functional male flowers are rudimentary, shriveled, and exhibit various stages of degeneration (Cai et al., 1993a, 1993b; Wetzstein et al., 2011; Chen et al., 2017a). Pomegranate flowers can contain several ovules, and the number of ovules varies widely with flower size (Wetzstein et al., 2011, 2013). The number of ovules in flowers is crucial because it can influence the aril

number and therefore fruit size in pomegranates. Excessive production of functional male flowers can also result in decreased yields due to their inability to set fruit (Wetzstein et al., 2013). Understanding the regulatory mechanisms underlying ovule number and development is essential, as these factors contribute to determine the number of seeds and final yield. Although the mechanism of ovule development has been elucidated in the model plant Arabidopsis, the mechanism in pomegranates is still unclear. The functions of ovule-related genes *CRC* and *INO* have not been reported in pomegranates, which dramatically limits the research on the mechanism of ovule development in pomegranates. Here, we cloned two YABBY genes (*PgINO* and *PgCRC*) in pomegranate, investigated their expression patterns, and determined their subcellular localization. We also used yeast two-hybrid (Y2H) assays, bimolecular fluorescence complementation (BiFC) assays, and ectopic transformation to predict the functions of genes in the formation of floral organs and the development of seeds.

Results

Ovule morphology in bisexual and functional male flowers of pomegranate

To determine the status of ovule sterility in pomegranate functional male flowers, we observed the dynamic development of ovules in bisexual and functional male flowers at different developmental stages. Bisexual flowers were vase shaped, whereas functional male flowers were bell shaped (Figure 1). Ovule primordia were formed when the vertical diameter of the flowers was 3.0–5.0 mm (Figure 2, A and F). When the vertical diameter was 5.1–8.0 mm, the ovules of bisexual flowers were larger than those of functional male flowers (Figure 2, B and G). The outer and inner integument primordia formed in bisexual flowers with a vertical diameter of 8.1–10.0 mm, and the ovule grew parallel to the nucellus through anticlinal cell division and elongation (Figure 2C). However, the integument primordia were not observed in functional male flowers (Figure 2H). When the vertical diameter was 10.1–13.0 mm, the outer integument grew rapidly and completely enclosed the inner integument in bisexual flowers (Figure 2D). Many of the ovules contained megaspore archesporial cells or megaspore mother cells (Figure 2K). In contrast, functional male flowers with a vertical diameter of 10.1–13.0 mm did not exhibit inner integument extension or outer integument primordia, megaspore mother cells were not observed, and their ovules showed curved growth paralleled to the placenta (Figure 2I). Mature ovules were visible in bisexual flowers with a vertical diameter of 13.1–15.0 mm (Figure 2E). Integument primordia, megaspore archesporial cells and megaspore mother cells were not observed in functional male flowers; however, the ovules were rudimentary, shriveled, and severely degenerated (Figure 2, J and L). The results obtained from the paraffin sections of the flowers were consistent with those of a previous study
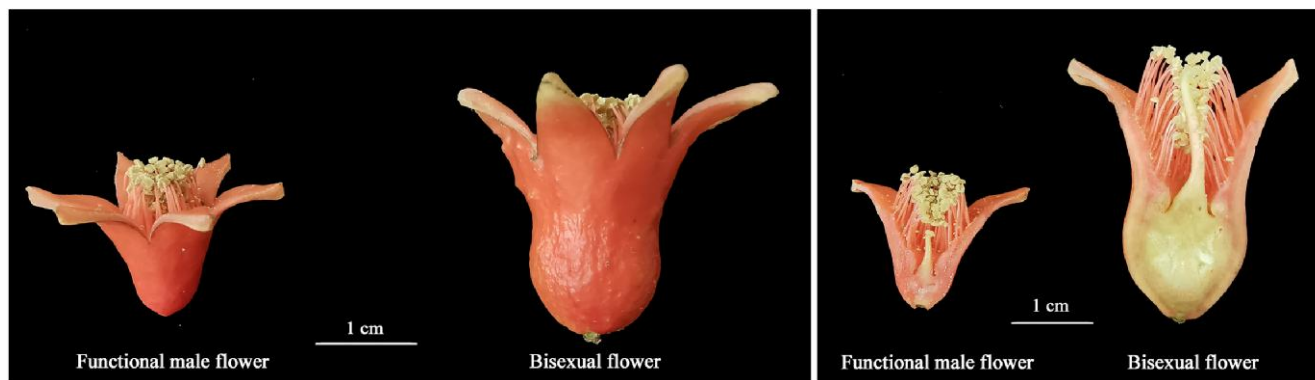
Figure 1 Morphology of bisexual and functional male flowers of pomegranate. Functional male flower was substantially smaller than bisexual flower. Functional male flower exhibited shortened pistils and rudimentary ovules. Bisexual flower possessed a well-developed pistil with an elongated style, and ovules were numerous and tightly packed.

(Cai et al., 1993a, 1993b; Wetzstein et al., 2011; Chen et al., 2017a), which confirmed the accuracy and reliability of our results. These results indicated that ovule integuments were unformed in pomegranate functional male flowers with a vertical diameter of 8.1–13.0 mm, resulting in female sterility; this indicated that this was a critical stage for pomegranate ovule development.

Ovule-related gene expression pattern analysis by transcriptome data of pomegranate flowers

According to Chen's study (2017) and the paraffin section results, we divided the pomegranate ovule development process into three stages (the first stage: 5.0–10.0 mm; the second stage: 10.1–13.0 mm; the third stage: 13.1–18.0 mm). At the first stage, ovules were involved in the initiation of integument primordia. At the second stage, the ovule integuments developed normally, the ovules were anatropous, and however, ovules showed curved growth paralleled to the placenta in functional male flowers. At the third stage, the mature ovules developed into seeds, the ovules of functional male flowers were rudimentary and severely degenerated. To examine the expression patterns of ovule-related genes during ovule sterility, we analyzed the transcriptome data of three stages of pomegranate flowers. RNA-Seq results showed that *PgAG* (the gene homologous to *AG* [*AGAMOUS*]) was highly expressed at the first stage and the third stage of bisexual flowers, and the second stage of functional male flowers (Figure 3). However, *PgAG* was weakly expressed at the second stage of bisexual flowers. *PgANT*, *PgCRC*, and *PgSEP3b*
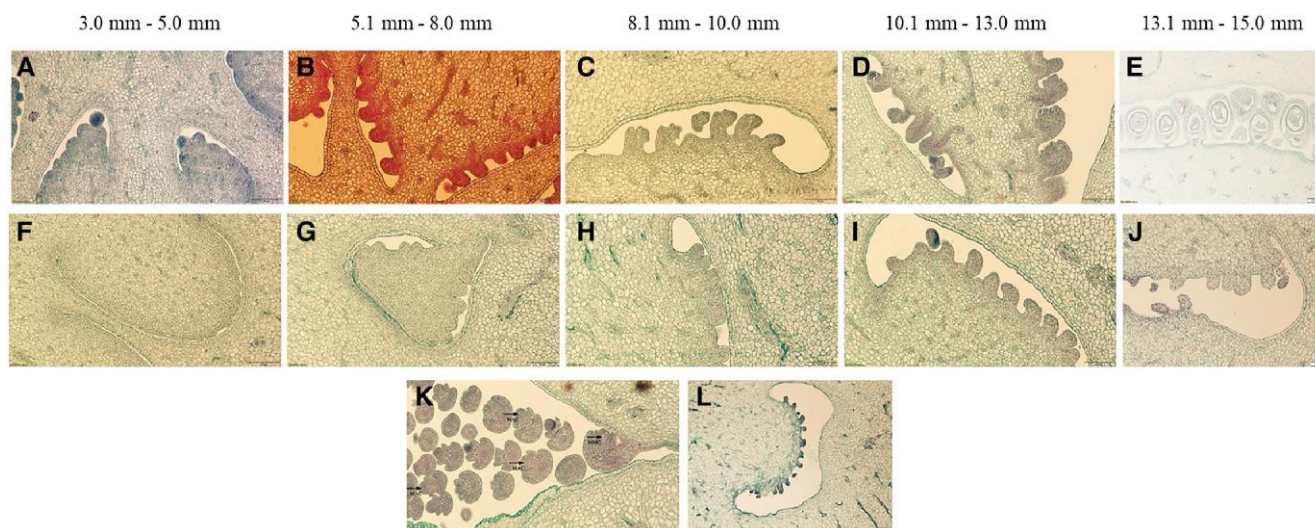

Figure 2 Morphology of ovules during ovule development in bisexual and functional male flowers of pomegranate. The ovule morphology of flowers when their bud vertical diameter was 3.0–5.0, 5.1–8.0, 8.1–10.0, 10.1–13.0, and 13.1–15.0 mm, were observed by paraffin section. A–E, The ovule morphology of bisexual flowers; A/C/D, bars = 50 μm; B, bar = 200 μm; and E, bar = 100 μm. F–J, The ovule morphology of functional male flowers; F–I, bars = 50 μm; J, bar = 100 μm. K, The ovule morphology of bisexual flowers (10.1–13.0 mm); MAC, megaspore archesporial cell; MMC, megaspore mother cell, bar = 50 μm. L, The ovule morphology of mature functional male flowers (15.1–18.0 mm), bar = 100 μm.
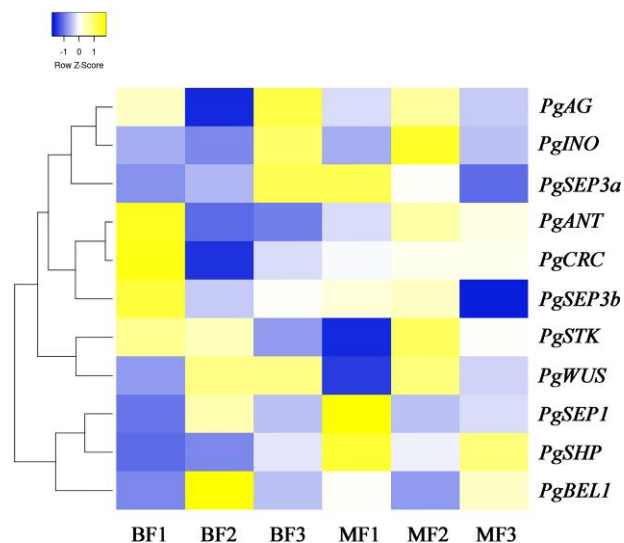
Figure 3 The heatmap of ovule-related genes in pomegranate flowers. BF1, BF2, and BF3 represented pistil of bisexual flowers when their bud vertical diameter was 5.1–10.0, 10.1–13.0, and 13.1–18.0 mm, respectively. MF1, MF2, and MF3 represented pistil of functional male flowers when their bud vertical diameter was 5.1–10.0, 10.1–13.0, and 13.1–18.0 mm, respectively.

Figure 4 Phylogenetic tree of different species based on the amino acid sequences of INO. Phylogenetic tree of INO putative orthologs in various plant species. Monocotyledons: Os, *Oryza sativa*; Zm, *Zea mays*. Dicotyledons: At, *Arabidopsis thaliana*; Atri, *Amborella trichopoda*; Na, *Nymphaea alba*; Nc, *Nymphaea colorata*; Eg, *Eucalyptus grandis*; Pgr, *Punica granatum* (Dabenzi); Zj, *Ziziphus jujuba*; Pv, *Pistacia vera*; Cc, *Citrus clementina*; Cs, *Citrus sinensis*; Sly, *Solanum lycopersicum*; Vv, *Vitis vinifera*. Rosidae plants: Rc, *Rosa chinensis*; Pd, *Prunus dulcis*; Pa, *Prunus avium*; Md, *Malus domestica*; Par, *Prunus armeniaca*; Ppe, *Prunus persica*. The accession numbers of those genes are included in Supplemental Table 1. The bar indicates 0.05 aa substitutions per site.

(the gene homologous to *SEPALLATA*) were highly expressed at the first stage, but *PgSTK* (*SEEDSTICK* orthologous gene) was strongly expressed at the first and second stages of bisexual flowers. In functional male flowers, *PgSTK* transcriptional level of the second stage was higher than that of the first and third stages. *PgSEP1* was highly expressed at the first stage of functional male flowers and the second stage of bisexual flowers. *PgWUS* was highly expressed at the second and third stages of bisexual flowers and the second stage of functional male flowers. *PgBEL1* (*BELL1* orthologous gene) was strongly expressed at the second stage of bisexual flowers. Interestingly, *PgCRC* was only expressed at the stage of integument development (5.1–10.0 mm). Therefore, we further explored the function of *CRC* in pomegranate pistils.

Phylogenetic relationships among the INO and CRC proteins in different species

To better understand the relationship between INO proteins in pomegranate and other plants, we conducted phylogenetic analyses using the sequences of 19 proteins homologous to INO and the pomegranate INO (Supplemental Table 1). INO proteins from dicotyledons and monocotyledons clustered independently, in line with their highest phylogenetic distance (Figure 4). The pomegranate INO protein clustered closer to the eucalypt (*Eucalyptus grandis*) protein, whereas INO proteins from Rosidae including apple (*Malus domestica*) and almond (*Prunus dulcis*) grouped as a separate clade. The Rosidae plants were mostly mononuclear seed fruits located at the top of the evolutionary tree. Maize (*Zea mays*), tomato (*Solanum lycopersicum*), and Arabidopsis showed polyovule and polyseed traits, which were similar to the traits in
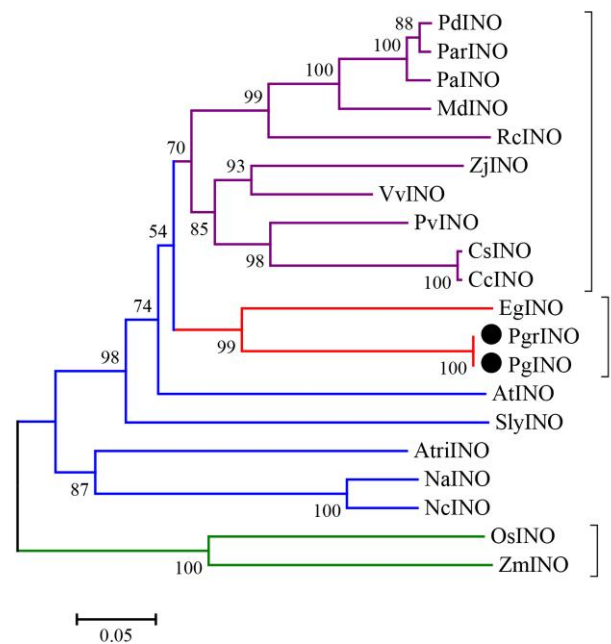
pomegranate. Moreover, these taxa were located at the base of the evolutionary tree, indicating that the function of PgINO was relatively conserved.

The phylogeny of known *CRC* genes was reconstructed using the amino acid sequences of respective genes (Supplemental Table 2). Gymnosperms and Gramineae were successfully classified and clustered distantly to the pomegranate protein. The PgCRC clusters were more closely related to the *E. grandis* sequence located at the top of the evolutionary tree (Figure 5). Overall, the conserved protein sequence of our limited sample of CRC protein sequences was consistent with the recently reported phylogenies of dicot species (Orashakova et al., 2009).

Subcellular localization analysis

To analyze the subcellular localization of PgINO and PgCRC, the CDSs of PgINO and PgCRC were ligated upstream of a green fluorescent protein (GFP) tag under the control of the 35S promoter, and the genes were overexpressed in *Nicotiana benthamiana* leaves using *Agrobacterium tumefaciens*-mediated transformation (Figure 6). As a control, the GFP fluorescence signal was found to be present in both cytoplasm and nuclei. The fluorescence signals of
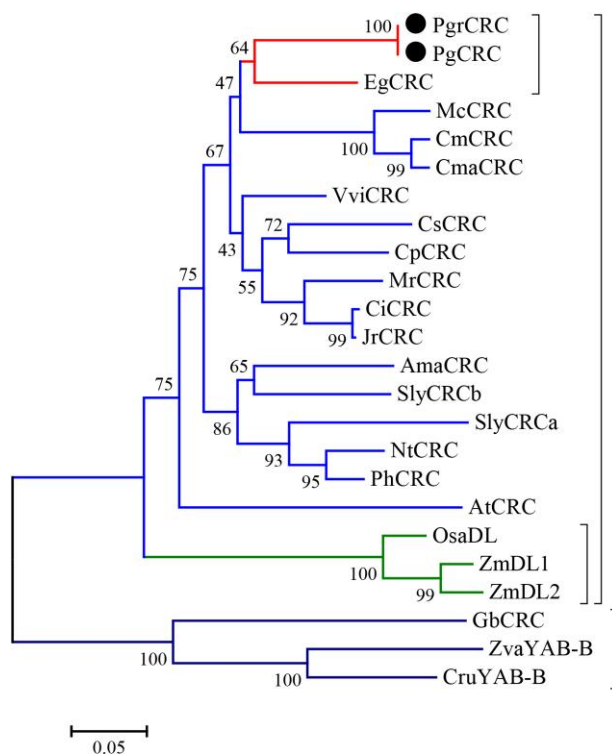
Figure 5 Phylogenetic tree of different species based on the amino acid sequences of CRC. Phylogenetic reconstruction of CRC putative orthologs in various plant species. Gymnosperms: ZvaYAB-B, *Zamia vazquezii*; CruYAB-B, *Cycas rumphii*; GbCRC, *Ginkgo biloba*. Gramineae: OsaDL, *Oryza sativa*; ZmDL1 and ZmDL2, *Zea mays*. Dicotyledons: At, *Arabidopsis thaliana*; Sly, *Solanum lycopersicum*; Ph, Petunia × hybrida; Ama, *Antirrhinum majus*; Nt, *Nicotiana tabacum*; Vvi, *Vitis vinifera*; Cm, *Cucurbita moschata*; Mr, *Morella rubra*; Eg, *Eucalyptus grandis*; Cma, *Cucurbita maxima*; Mc, *Momordica charantia*; Ci, *Carya illinoinensis*; Jr, *Juglans regia*; Pgr, *Punica granatum* (Dabenzi); Cs, *Citrus sinensis*; Cp, *Carica papaya*. The accession numbers of those genes are included in Supplementary Table 2. The bar indicates 0.05 aa substitutions per site.

PgINO::GFP and PgCRC::GFP fusion protein were located in the nuclei, indicating that PgINO and PgCRC functioned in the cell nucleus.

Functional analysis of the pomegranate *INO*
Tissue-specific expression analysis of *PgINO* in pomegranates showed that *PgINO* expression level of bisexual flowers was higher than that of functional male flowers during flower development (Zhao et al., 2020a). When the bud vertical diameter was 10.1–12.0 mm, the expression level of *PgINO* in bisexual flowers was 5.3 times higher than that in functional male flowers. *PgINO* transcriptional level in bisexual flowers was 2.0 times higher than that in functional male flowers at a bud vertical diameter of 5.1–8.0 mm, 3.9 times at 8.1–10.0 mm, and 1.1 times at 12.1–14.0 mm.

In *ino* mutant plants, ovule development is similar to WT development until Stage 2-III, at which time the outer integument fails to initiate. The inner integument is unaffected and

envelops the nucellus by Stage 4-I, and there is an absence of outer integument growth on both sides of the ovule primordium. *ino* mutations caused no visible alterations in other aspects of ovule, flower, or vegetative development (Villanueva et al., 1999). Recent experiments in solanaceous species demonstrated that *SlINO* was not able to complement the Arabidopsis *ino* mutant (Skinner et al., 2016). To determine whether ectopic *PgINO* expression was sufficient to induce ovule and seed development, Arabidopsis plants were transformed with a chimeric gene construct in which the *PgINO* cDNA coding region was fused with the 35S enhancer promoter (Figure 7, D–I). The inflorescence morphology and bud number of 35S::*PgINO* lines were consistent with those of the WT (Figure 7, A and D). In contrast, the number of buds in 35S::*PgINO*/*ino* lines (complemented *ino* mutant) was substantially lower than that in WT (Figure 7, A and G). The siliques morphology of the 35S::*PgINO* and 35S::*PgINO*/ *ino* lines was similar to that of WT (Figure 7, B, E, and H). Both the *PgINO* overexpression line and the *ino* complement line showed leaf tips and a marked reduction, but the leaf shape was not substantially different between the transgenic lines and WT (Figure 7, C, F, and I). The average seed number of the35S::*PgINO* silique was 34.8 (Figure 7P), which was significantly higher than that of WT (average: 26 seeds). The seed number of per silique was higher in 35S::*PgINO*/*ino* than that in WT, but the difference was not significant (Figure 7P). *PgINO* successfully rescued the seeds set in the Arabidopsis *ino* mutant, which was consistent with the result of *VviINO* in *V. vinifera* ovule development and seed formation (di Rienzo et al., 2021). The ectopic expression results showed that *PgINO* promoted an increase in the number of seeds, indicating that *PgINO* is involved in ovule primordia formation.

Next, we evaluated the expression regions of *PgINO* and determined the outer integument growth of ovules and seed set (di Rienzo et al., 2021). We found that β-glucuronidase (GUS) was expressed in the buds, petals, fruits, and seed coat of the 35S::*PgINO* transgenic line (Figure 8, A–D). GUS staining of the 35S::*PgINO*/*ino* lines showed that *PgINO* was expressed in the buds and young fruits and weakly expressed in mature fruits, but not in the leaves (Figure 8, E–G), indicating that *PgINO* may be involved in the development of flower organs and seeds.

Functional analysis of the pomegranate *CRC*
In a previous study, we reported that *PgCRC* expression level in bisexual flowers was higher than that in functional male flowers at the critical stage of ovule development (8.1–13.0 mm; Zhao et al., 2020a). When the bud vertical diameter was 8.1–10.0 mm, *PgCRC* transcriptional level in bisexual flowers was 1.5 times the level in functional male flowers. Moreover, *PgCRC* transcriptional levels in bisexual flowers were 2.1 and 2.4 times higher than that in functional male flowers buds with vertical diameters of 10.1–12.0 and 12.1–14.0 mm, respectively.
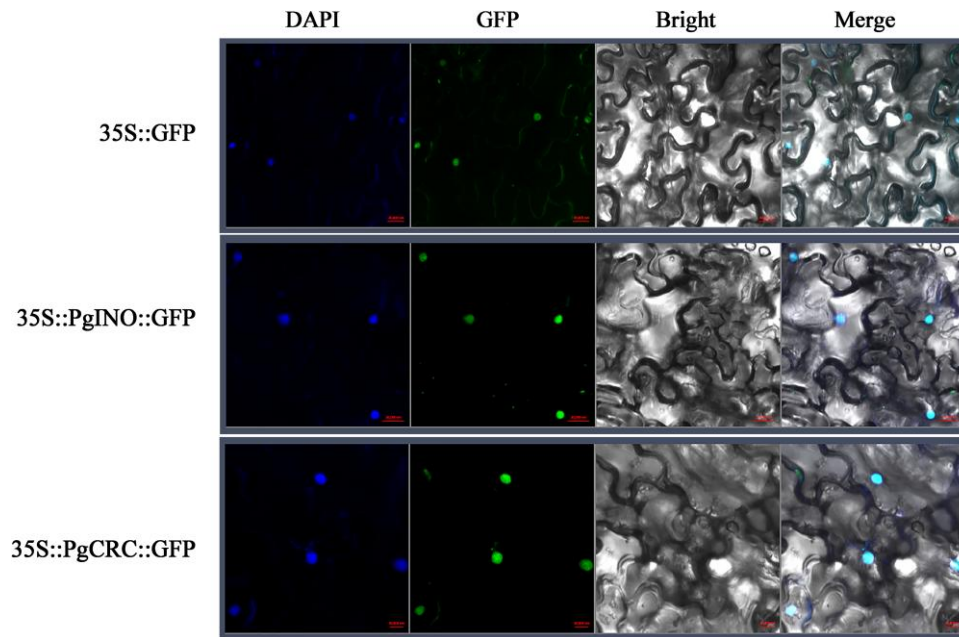
Figure 6 Subcellular localization of PgINO::GFP and PgCRC::GFP fusion proteins in *Nicotiana tabacum* cells. The empty 35S::GFP was a control in this assay, and expression signals mainly gathered in the cytoplasm and nuclei. Bars = 20 μm.

Tomato *CRC* paralogues *SlCRCa* and *SlCRCb* operate as positive regulators of floral meristem determinacy by acting in a compensatory and partially redundant manner to safeguard the proper formation of flowers and fruits (Castañeda et al., 2022). To explore the putative function of *PgCRC* in floral organ development, the 35S::*PgCRC* construct was introduced into Arabidopsis through *Ag. tumefaciens*-mediated transformation. The *crc* mutant flower

was similar to that of WT plants, except the carpels were not fused at the apical region (Bowman and Smyth, 1999). In *crc* mutant plants, the gynoecium is wider and shorter throughout development, contains fewer ovules, and has a reduced amount of style tissue (Alvarez and Smyth, 1999). The number of flower buds of the 35S::*PgCRC* and 35S::*PgCRC/crc* (complemented *crc* mutant) lines were substantially lower than that of WT (Figure 7, A, J, and M). The leaves of WT
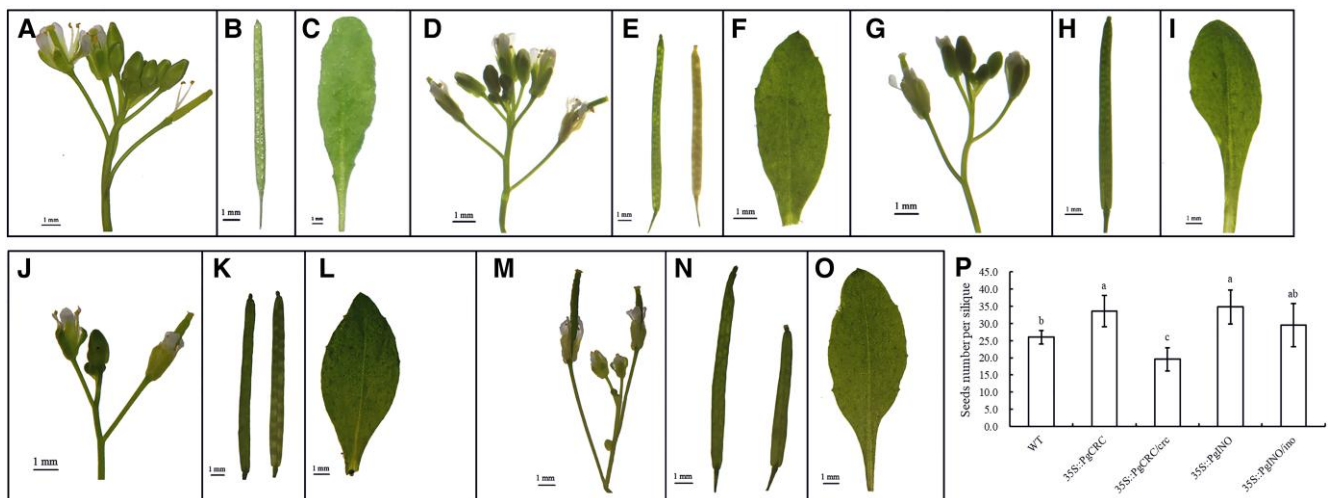

Figure 7 Phenotypic analysis of 35S::PgINO and 35S::PgCRC *Ar. thaliana* T3 plants. A–C, The inflorescence, silique, and leaf of WT. D–F, The inflorescence, siliques, and leaf of 35S::PgINO transgenic plants. G–I, The inflorescence, silique, and leaf of the transgenic ino mutant plant ectopically expressing PgINO. J–L, The inflorescence, siliques, and leaf of 35S::PgCRC transgenic plants. M–O, The inflorescence, siliques, and leaf of the transgenic crc mutant plant ectopically expressing PgCRC. Bars = 1 mm. P, The number of seeds in transgenic *Ar. thaliana* T3 plants. The fully developed siliques were randomly picked. Data were expressed as the mean ± SD, different letters indicated significant differences at $P < 0.05$ (Duncan's test, error bars represented the SD of five biological repeats.
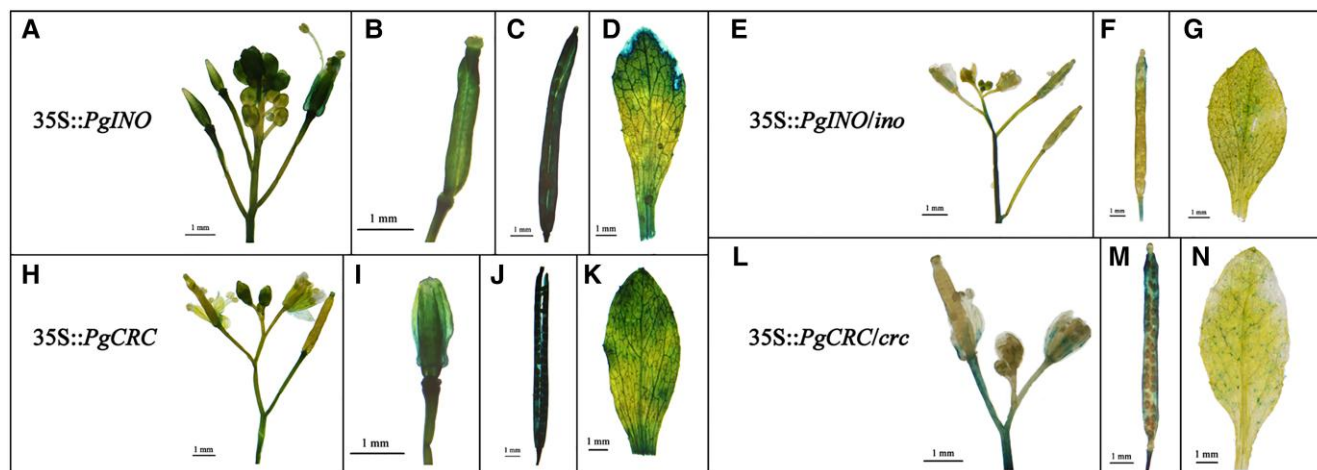
Figure 8 GUS staining analysis of different tissues in *Ar. thaliana* T3 of PgINO and PgCRC. A–D, The inflorescence, young silique, mature silique, and leaf of 35S::PgINO transgenic plants. E–G, The inflorescence, silique, and leaf of the transgenic ino mutant plant ectopically expressing PgINO. H–K, The inflorescence, young silique, mature silique, and leaf of 35S::PgCRC transgenic plants. L–N, The inflorescence, silique, and leaf of the transgenic crc mutant plant ectopically expressing PgCRC. Bars = 1 mm.

plants are long and elliptical with notches (Figure 7C). The *PgCRC* overexpression lines had elliptical leaves with obvious leaf tips and substantially reduced notches (Figure 7L). 35S::*PgCRC*/*crc* complemented plants had a blunt, round leaf tip, and elliptical leaf shape (Figure 7O). The siliques of *PgCRC* overexpression lines developed normally (Figure 7K), and the average seed number of siliques was 33.6 (Figure 7P), which was significantly higher than that of WT (average: 26 seeds). Some siliques of 35S::*PgCRC*/*crc* lines had developmental defects (Figure 7N), the seed number of per siliques was significantly lower than that in WT (Figure 7P). These results showed that *PgCRC* could partially complement the Arabidopsis *crc* mutant, which were similar to the results of *PeDL1* and *PeDL2* in orchid (Chen et al., 2021). Our results illustrated that *PgCRC* affected the number of seeds and contributed to ovule primordia formation.

To determine the expression pattern of *PgCRC*, we soaked the inflorescences, young fruits, mature fruits, and leaves of 35S::*PgCRC* transgenic lines in GUS staining solution. The tissues were then decolorized and photographed 24 h after staining. The results showed that the buds, young fruits, seeds, and seed coat of 35S::*PgCRC* transgenic lines had blue precipitates (Figure 8, H–K). GUS staining of *PgCRC* complemented transgenic lines showed that *PgCRC* was expressed in the petals and seed coat, but not in the leaves (Figure 8, L–N). Our results indicated that *PgCRC* expression promotes the development of the seed and seed coat.

Expression pattern of ovule identify genes in transgenic Arabidopsis

To explore the potential relationships between ovule identity genes in pomegranate, we investigated the expression patterns of *INO*, *CRC*, *BEL1*, and *SEEDSTICK* (*STK*) in stem, leaf, flowers, siliques of WT, and transgenic Arabidopsis lines (Figure 9). The

results showed that both *PgINO* and *AtINO* were predominantly expressed in siliques (Figure 9A). In addition, transcripts of *AtINO* could be specifically detected in flowers and young leaf. *PgINO* was hardly expressed in vegetative tissues, such as stem and leaves. In young siliques, the expression levels of *PgINO* in transgenic lines were significantly higher than *AtINO* in WT. During siliques development in the 35S::*PgINO* transgenic lines, *PgINO* transcriptional level of young and mature siliques were 1.6 and 0.97 times that *AtINO* levels of siliques, respectively. In *PgINO* complemented *ino* transgenic lines, *PgINO* transcription level of young siliques was 2.03 times higher than that of mature siliques. These results suggested that *PgINO* was involved in siliques development, indicating that *PgINO* may regulate seed number.

We determined the mRNA expression patterns of *PgCRC* in WT, 35S::*PgCRC* transgenic lines, and 35S::*PgCRC* complemented *crc* mutant lines (Figure 9B). *PgCRC* was hardly expressed in stem and leaves of transgenic lines. In flowers, transcripts of *AtCRC* were higher than *PgCRC* in transgenic lines. Transcript of *PgCRC* was strongly detected in the siliques of *PgCRC* complemented *crc* mutant lines, which were significantly higher than *AtCRC* in WT. During siliques development of the 35S::*PgCRC* transgenic lines, the mRNA levels of *PgCRC* in young and mature siliques were 12.2 and 0.71 times of *AtCRC* level in WT siliques, respectively. In 35S::*PgCRC*/*crc* transgenic lines, the expression of *PgCRC* in siliques was higher than that in flowers and stems, young siliques was 1.19 times higher than that in mature siliques. These results suggested that *PgCRC* was involved in siliques development.

To clarify the expression patterns of *AtBEL1* in the transgenic lines and WT, we performed reverse transcription-quantitative polymerase chain reaction (RT-qPCR) analyses (Figure 9C). The expression of *AtBEL1* was strongly detected in mature siliques of WT and mature leaf of 35S::*PgINO*
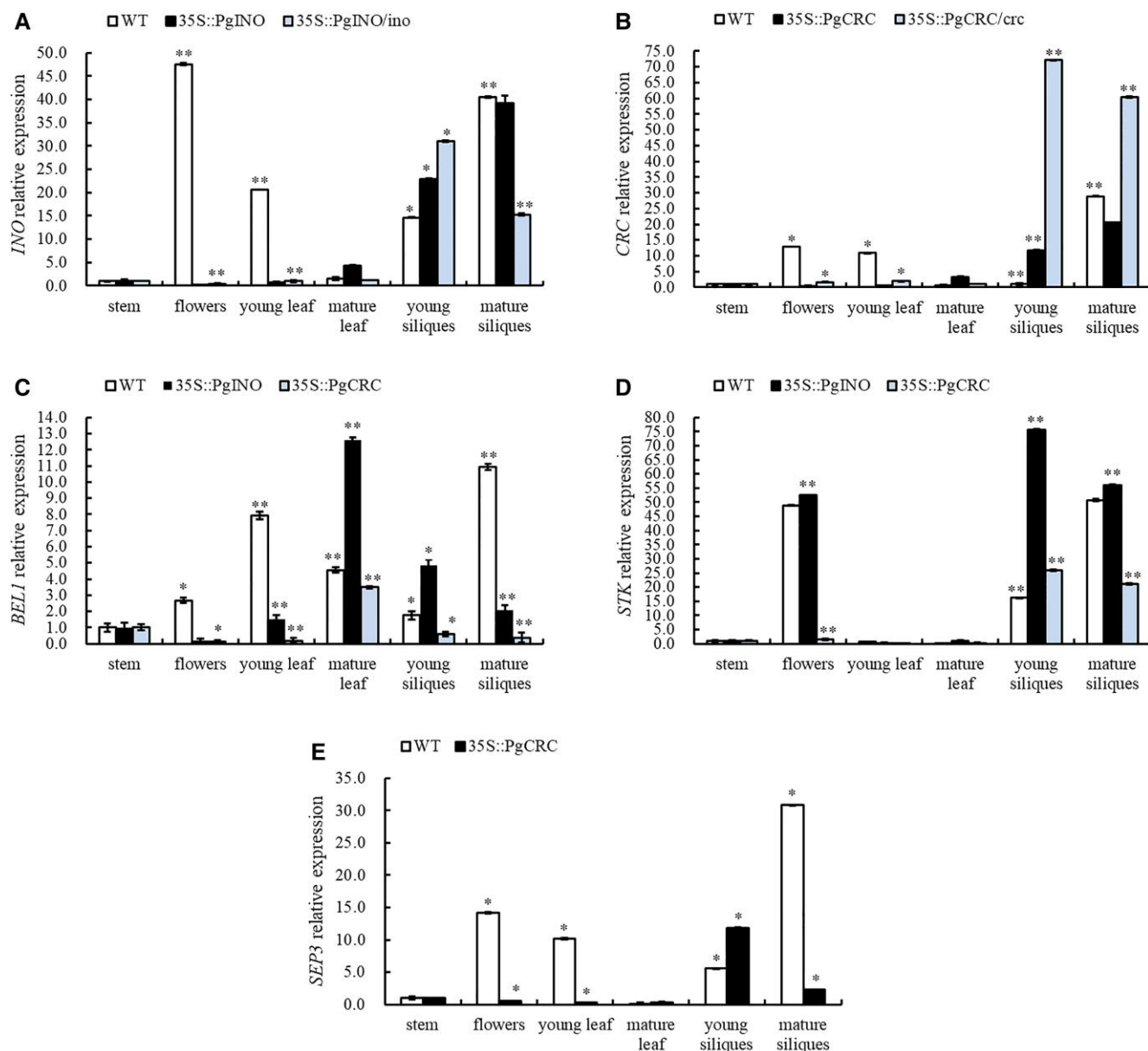
Figure 9 Expression patterns of ovule identify genes in WT, 35S::*PgINO* and 35S::*PgCRC* Arabidopsis transgenic plants. A, *INO* expression in WT, 35S::*PgINO* and 35S::*PgINO/ino* plants. B, *CRC* expression in WT, 35S::*PgCRC* and 35S::*PgCRC/crc* plants. C, *BEL1* expression in WT, 35S::*PgINO* and 35S::*PgCRC* plants. D, *STK* expression in WT, 35S::*PgINO* and 35S::*PgCRC* plants. E, *SEP3* expression in WT and 35S::*PgCRC* plants. Several pre-bloom flowers were collected for each transgenic line. Stem, leaf, and young siliques were collected at the same time. Mature siliques were collected when seed coat turned yellow. Data were means ± SD of three technical replicates. * represented the level of significance difference $P < 0.05$, ** represented the level of significance difference $P < 0.01$ in independent-samples t-test (Refer to Chen et al., 2017a).

transgenic lines. In contrast, *AtBEL1* was not expressed in flowers of the transgenic lines. In flowers and mature siliques, *AtBEL1* transcriptional level of WT was significantly higher than that of transgenic lines. In young siliques, the expression levels of *AtBEL1* in 35S::*PgINO* transgenic lines were higher than that in WT, this result suggested that *PgINO* promoted *AtBEL1* expression at the transcript level in young siliques development.

The expression patterns of *AtSTK* in the transgenic lines and WT were analyzed by RT-qPCR (Figure 9D). The expression of *AtSTK* was strongly detected in siliques and flowers. In contrast, *AtSTK* was hardly expressed in leaf and stem. The transcription levels of *AtSTK* in young and mature siliques of the 35S::*PgINO* transgenic lines were 4.7 and 1.1 times the levels of WT, respectively. These results suggested that *PgINO* promoted *AtSTK* expression at the transcriptional level during siliques development.

In 35S::*PgCRC* transgenic lines, *AtSEP3* was hardly expressed in stem, flowers, and leaves (Figure 9E). In 35S::*PgCRC* transgenic lines, *AtSEP3* transcription levels of young and mature

siliques were 2.1 and 0.07 times of the levels in WT, respectively. Our comparative analyses showed that *PgCRC* activity was required for the activation of *AtSEP3* expression at the transcript level in young siliques.

PgINO and PgCRC interacted with the ovule identity protein, PgBEL1

To examine the genetic interactions between PgINO, PgCRC, and ovule identity protein BEL1, we performed Y2H assay with a gene CDS to elucidate the formation of homodimers for this protein–protein interaction. The results showed that PgCRC could directly interact with PgBEL1, and PgINO was also able to interact with PgBEL1 (Figure 10). To confirm the interactions between the PgINO, PgCRC, and PgBEL1 proteins in vivo, we performed BiFC assays (Figure 11). YFP fluorescence was restored in the nuclei of *N. benthamiana* leaf cells when the pSPYNE-YFP tag of PgBEL1 was fused to pSPYCE-YFP-PgCRC/PgINO in the same orientation. The emitted YFP signals revealed that PgCRC and PgBEL1 could form heterodimers, and that the PgINO-PgBEL1 dimer could form in the nucleus. No YFP signal was observed in the controls in Supplemental Figure 1. These results indicated that PgBEL1 was able to interact with PgINO and PgCRC in pomegranate.

MADS-box transcription factors such as AGAMOUS (AG), STK, SHATTERPROOF (SHP1, SHP2), and SEP are known to regulate ovule identity and influence ovule initiation and development (Favaro et al., 2003; Pinyopich et al., 2003; Zhang et al., 2020). We determined that PgAG, PgSTK, and PgBEL1 interacted with SEPALLATA (PgSEP) proteins were located in the nuclei of *N. benthamiana* cells (Supplemental Figure 2). To identify the MADS-box members that could interact with PgCRC proteins, we performed Y2H assays with

PgCRC proteins as prey. Our results showed that PgCRC did not interact with the PgSTK, PgAG, and PgSEP proteins (Figure 10). Furthermore, the PgINO-PgAG, PgINO-PgSEP, and PgINO-PgSTK heterodimers did not occur in the Y2H assay on histidine drop-out medium (SD-His/Leu/Met/Trp; Figure 10), indicating that they could not directly interact with each other.

PgBEL1 interacted with the ovule identity proteins in the MADS-box family

The genetic relationships between the ovule identity genes *BEL1*, *AG*, and *STK* have been elucidated very recently with the characterization of the *bel1 stk shp1 shp2* quadruple mutant (Brambilla et al., 2007). Genetic and protein interaction studies have shown that AG, STK, SHP, and BEL1 interact with SEP to participate in ovule development (Favaro et al., 2003; Pinyopich et al., 2003). We performed interaction assays to explore whether PgBEL1 regulates MADS-box protein activity at the protein level. The results indicated that PgBEL1 was unable to interact with PgAG and PgSTK on histidine drop-out medium (SD-His/Leu/Met/Trp; Figure 10).

SEP is essential for normal ovule development, and SEP proteins participate in the formation of higher order transcription factor complexes consisting of various combinations of MADS-box proteins (Vandenbussche et al., 2003). Without SEP-like proteins, the ovule identity complex cannot be formed, and the ovule identity pathway cannot be initiated (Immink et al., 2009). Our results revealed that PgSEP1 interacted with PgAG, PgSTK, and PgBEL1 (Figure 12). Likewise, PgSEP4 proteins could directly interact with PgAG, PgSTK, and PgBEL1. To confirm the observed interactions in yeast, we performed BiFC assays to demonstrate that PgSEP1/4
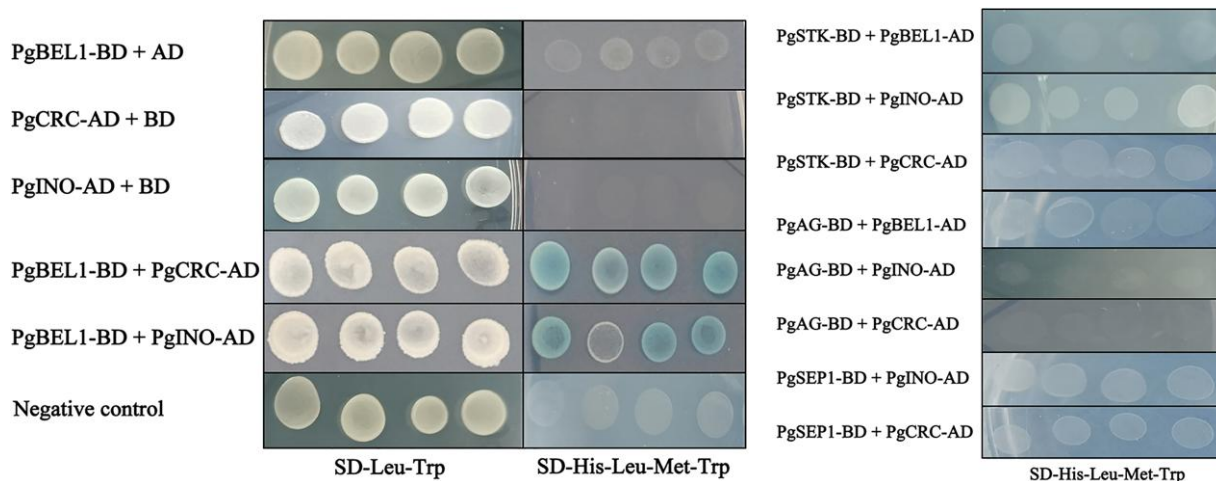

Figure 10 Interaction assays to test for interactions between PgINO, PgCRC, PgBEL1, and MADS-box proteins. Yeast cell suspensions of the respective test strains plated on SD-Leu-Trp medium and stained with X-α-Gluc after 5 days of incubation and on SD-His-Leu-Met-Trp + 3 mM 3-AT with X-α-Gluc. There were four repeats for each sample. As positive control, the combination of PgINO-AD-BD/PgCRC-AD-BD/PgBEL1-AD-BD were used and a combination of the empty vectors pGADT7/pGBKT7 as negative control.
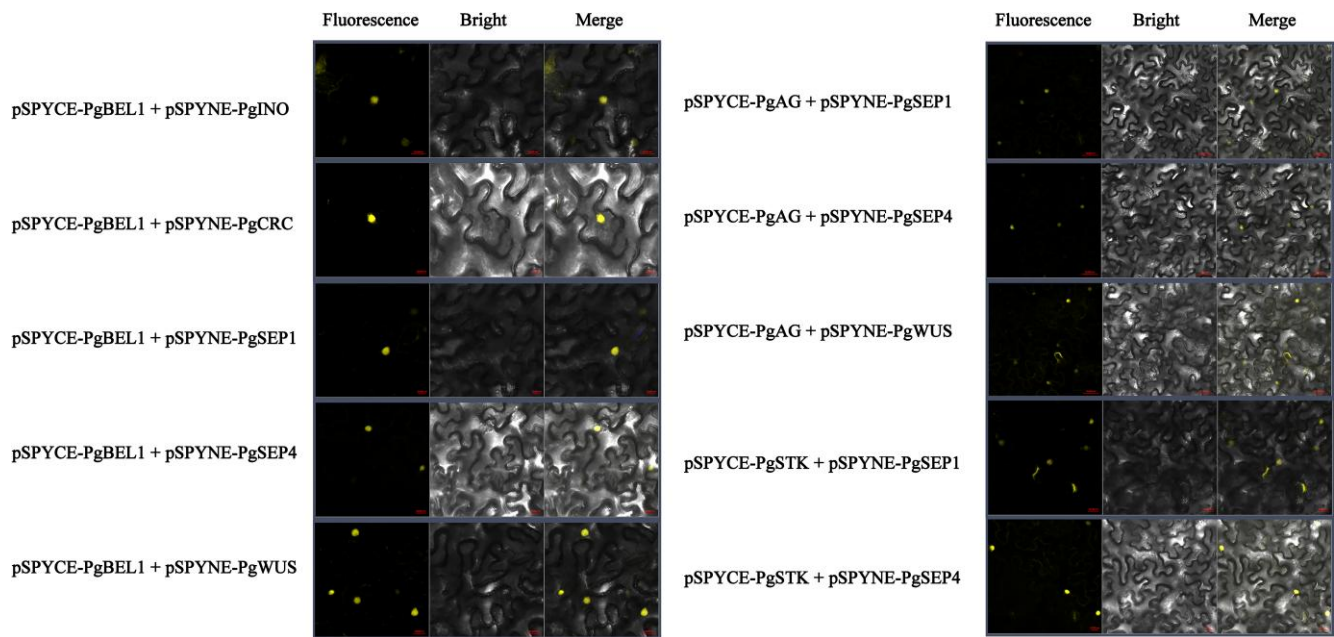
Figure 11 BiFC assays to verify protein interactions. BiFC images showed in vivo interactions in *Nicotiana tabacum* leaves between the yellow fluorescent protein (YFP) C-terminal region fused to PgBEL1 (pSPYCE-PgBEL1), PgAG (pSPYCE-PgAG), and PgSTK (pSPYCE-PgSTK), and fusions of the YFP N-terminal region fused to PgINO (pSPYNE-PgINO), PgCRC (pSPYNE-PgCRC), PgSEP1 (pSPYNE-PgSEP1), PgSEP4 (pSPYNE-PgSEP4), PgWUS (pSPYNE-PgWUS). As negative control, each protein under study was fused to pSPYCE or pSPYNE. Scale bars = 50 μm, Scale bars = 20 μm (PgBEL1-PgCRC).

proteins formed heterodimers with PgAG, PgSTK, and PgBEL1 (Figure 11). Our results indicated that although PgBEL1 did not directly interact with PgSTK and PgAG, PgSEP acts as a molecular bridge linking PgBEL1 and MADS-box transcription factors to regulate pomegranate ovule development.

Discussion

Morphology of ovule development in pomegranates

Pomegranate pistils contain the ovaries, styles, and stigma, and the ovules in pomegranate flowers have two-layered integuments. The inner integument comprises 2–3 cell layers, but the outer integument is even thicker (Wetzstein et al., 2011). Ovules are essential organs for sexual reproduction in plants, and the integuments develop into the seed coat during seed development (Lora et al., 2015). Our microscopic analyses showed that buds with a vertical diameter of 8.1–13.0 mm were the key stage for ovule sterility in functional male flowers. At this stage, the ovule integuments developed normally, and megaspore archesporial cells and megaspore mother cells were observed in bisexual flowers. However, the ovules of functional male flowers ceased development following the formation of the integument primordia. The megaspore mother cell is formed and goes into meiosis in bisexual flowers of "Pink" and "Green" pomegranate cultivars (Cai et al., 1993b). Our results were in agreement with those of a previous study reporting that in "Tunisiruanzi" plants, ovule development ceased in

functional male flowers with a vertical diameter of 5.0–13.0 mm (Chen et al., 2017a).

Molecular studies of ovule and integument development can help elucidate the pathways of ovule and seed development in pomegranates. The genetic pathways and regulatory mechanisms involved in ovule development have primarily been studied in *Ar. thaliana*, leading to the identification of several ovule identity genes (McAbee et al., 2006; Brambilla et al., 2007; Kelley et al., 2012; Skinner et al., 2016). One of the genes involved in ovule development is *INO*, which is expressed exclusively in the outer integument and is essential for the curvature of the ovule in *Ar. thaliana* (Siegfried et al., 1999; Villanueva et al., 1999). *CRC* is involved in the development of the placenta, nectary and carpel, and in ovule primordia initiation (Battaglia et al., 2009; Gross et al., 2018). Another crucial factor determining the identity and development of integuments is BEL1 (Reiser et al., 1995), which is required for proper morphogenesis of the ovule integuments. *BEL1* is expressed throughout the young ovule primordia, and is limited to the central region prior to the initiation of the integuments (Western and Haughn, 1999). We performed a comparative transcriptomic analysis between bisexual and functional male flowers to identify candidate genes involved in ovule development in pomegranates. We found that the ovule-related genes *INO*, *BEL1*, and *CRC* and MADS-box transcription factors were differentially expressed at the critical stage of pistil abortion (bud vertical diameter: 5.0–10.0 mm). *PgANT* and *PgSEP3b* were gradually downregulated in bisexual flowers, whereas *PgINO* and *PgWUS*
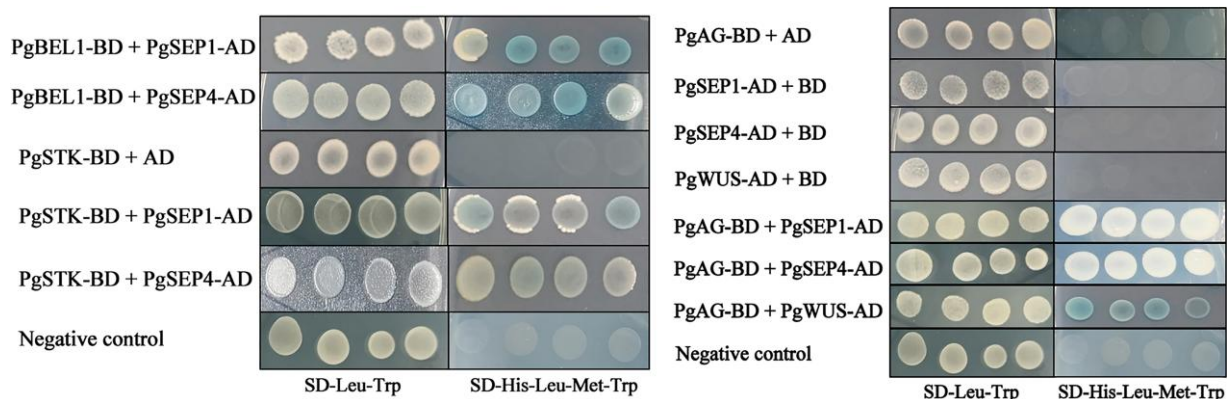
Figure 12 Interaction assays to test for interactions between PgBEL1 and MADS-box proteins. Yeast cell suspensions of the respective test strains plated on SD-Leu-Trp medium and stained with X-α-Gluc after 5 days of incubation and on SD-His-Leu-Met-Trp + 3 mM 3-AT with X-α-Gluc. There were four repeats for each sample. PgSTK-BD-AD/PgAG-BD-AD/PgSEP1-AD-BD/PgSEP4-AD-BD were used as the positive control, and a combination of the empty vectors pGADT7/pGBKT7 as negative control. The negative control images are the same within this figure and in Figure 10.

were upregulated, indicating that these genes were involved in the regulation of ovule development in pomegranates. Moreover, the genes homologous to *INO* and *ANT* were downregulated in functional male flowers at the key stage when ovule development ceased in "Tunisiruanzi" plants (Chen et al., 2017a). At the critical stages of pomegranate ovule sterility (5.1–12.0 mm), *PgBEL1* transcription level in bisexual flowers were higher than that in functional male flowers (Zhao et al., 2021), and this result was consistent with our study. Previous studies have confirmed the essential role of *PgAGL11* (*AGAMOUS-LIKE 11* orthologous gene) in female sterility in pomegranates (Chen et al., 2017b). At the key stage of pistil abortion, *PgCRC* and *PgSTK* were highly expressed in bisexual flowers and not in functional male flowers, indicating that these genes play essential roles in ovule development in pomegranates.

The pomegranate *CRCs* were needed for flower and seed development

CRC exists as a single copy in most angiosperms apart from Solanaceae, where *CRC* occurs as paralogous pairs due to a Solanaceae-α hexaploidy event (Phukela et al., 2020). In *Petunia hybrida*, the mRNAs of both *CRC1* and *CRC2* occur at the base of the ovary and nectary (Morel et al., 2018). Two *DL/CRC*-like genes have been shown to exhibit functional differences in ovule initiation in orchids (Chen et al; 2021). In *Eschscholzia californica*, *EcCRC* has been shown to control meristem determinacy, carpel polarity, and ovule initiation (Orashakova et al., 2009). Thus, CRC appears to have a conserved function, and is involved in the development of the carpel and nectary as well as ovule initiation (Lee et al., 2005; Orashakova et al. 2009; Chen et al., 2021). In a previous study, we identified *PgCRC* as the gene orthologous to *CRC* in pomegranates (Zhao et al., 2020a). Multiple sequence alignment and phylogenetic analysis showed that the pomegranate CRC protein and the *E. grandis* homolog clustered in one branch, distant from the protein in grapes (*V. vinifera*) and

walnuts (*Juglans regia*). Our results are consistent with those of Phukela et al. (2020). The subcellular localization patterns indicated that the PgCRC protein was located in the nucleus and had typical subcellular localization characteristics of the transcription factor, which was consistent with the results of a previous study reporting SlCRCa, SlCRCb, and PFCRC (*Physalis floridana CRABS CLAW*) localization in the nucleus (Gong et al., 2021; Castañeda et al., 2022).

In our previous study, we had demonstrated that *PgCRC* expression levels decreased with flower maturation in pomegranates. The transcription level of *PgCRC* was higher in bisexual flowers than in functional male flowers (bud vertical diameter: 8.1–14.0 mm; Zhao et al., 2020a). The style was shorter in functional male flowers with rudimentary ovules, and *PgCRC* was downregulated in functional male flowers at the critical stage for ovule sterility. The phenotype and *PgCRC* expression pattern of functional male flowers in pomegranate were consistent with the result of a previous study showing that *PsCRC* downregulation caused defects in carpel fusion and style/stigma development in pea (*Pisum sativum*; Fourquin et al., 2014). These results suggested that *PgCRC* plays an important role in pistil development, which is consistent with a previous report showing that *EcCRC* is involved in pistil and ovule differentiation (Orashakova et al., 2009).

To obtain further functional clues, we generated 35S::*PgCRC* transgenic lines. The 35S::*PgCRC* transgenic lines had 33.6 seeds per capsule, which was higher than that of WT. *PgCRC* was expressed in the inflorescences, seeds, and seed coats, indicating that *PgCRC* is involved in seed development. The ectopic expression of *PgCRC* did not cause the development of ectopic nectaries, which is consistent with the results of previous studies (Baum et al., 2001). Compared with WT, *crc* mutants produce carpels that are only partially fused together to form gynoecia. These eventually form siliques, which are considerably shorter and wider in *crc* mutants than in WT (Fourquin et al., 2007). The seed number of 35S::*PgCRC* complemented *crc* mutant lines per capsule was lower than that of WT, and the seeds at the top of the

siliques were degraded. Furthermore, the leaves of *PgCRC* complemented *crc* mutant lines were noticeably different from those of WT, and *PgCRC* could not completely restore the leaf shape of the *crc* mutant. These suggested that *PgCRC* might function similarly to homologous genes in the YABBY family, which are involved in leaf shape development (Siegfried et al., 1999), and *PgCRC* could not complement the phenotypic of Arabidopsis *crc* mutant. In orchids, *PeDL* genes are specifically expressed during the early stages of ovule development, and *PeDLs* affect the number of ovules differentiated from the placenta (Chen et al., 2021). RT-qPCR analysis showed that *PgCRC* was specifically expressed in siliques, and that its expression levels of 35S::*PgCRC* transgenic lines increased with siliques development. *PgCRC* overexpression was known to affect the number of ovules that develop into seeds. Our results were consistent with reports that *PFCRC* and *PeDL* alter the ovule number (Chen et al., 2021; Gong et al., 2021), suggesting that *PgCRC* is involved in the regulation of ovule and seed development.

Previous genetic analyses have shown that *CRC* is a direct target of *AG* (Lee et al., 2005; Ó'Maoiléidigh et al., 2013). In the floral meristem, AG can activate the expression of *CRC* (Bowman and Smyth, 1999; Ming and Ma, 2009). The MADS-box transcription factors AG, PI (PISTILATA), AP1 (APETALA1), and AP3 (APETALA3) directly bind to the *CRC* promoter. AG activates *CRC* expression in the developing flower, and PI, AP1, and AP3 restrict *CRC* to the nectary and carpel (Gómez-Mena et al., 2005; Lee et al., 2005; Ó'Maoiléidigh et al., 2013). To test whether there was a regulatory relationship between *CRC* and MADS-box ovule identity genes, we screened the target protein of PgCRC in pomegranate proteins. We found that PgAG, PgSEP and PgSTK were unable to interact with PgCRC, suggesting that PgCRC could not interact with MADS-box transcription factors to regulate ovule and floral organ development in pomegranates. Interestingly, our protein interaction analysis showed that PgCRC formed homodimers and interacted with PgBEL1. A study by Gong et al. (2021) had revealed that *CRC* mediates the neofunctionalization of *GLOBOSA* (*GLO*) and floral B-function MADS-box genes in carpel and ovule development. Moreover, Xu et al. (2019) analyzed the transcriptome of physic nut (*Jatropha curcas*) flower buds and found that *CRC* is involved in ovule development. Taken together, the results of protein interaction and genetic analyses indicated that *PgCRC* was involved in ovule formation and seed development in pomegranates by forming the PgCRC-PgBEL1 dimer.

Function of the pomegranate *INO* in flower and seed development

INO is essential for the formation and asymmetric growth of the outer integument of ovules (Villanueva et al., 1999). It also plays a crucial role in safeguarding reproduction by repressing NATURAL RESISTANCE-ASSOCIATED MACROPHAGE PROTEIN 1 (*NRAMP1*) expression to reduce Fe loading into developing seeds (Sun et al., 2021). In a previous study, we analyzed the expression patterns of *PgINO* to explore the expression differences of *PgINO* in bisexual and functional male flowers. *PgINO* expression level in bisexual flowers was higher than that in functional male flowers, and *PgINO* expression showed an upward trend in bisexual flowers (bud vertical diameter: 3.0–14.0 mm; Zhao et al., 2020a). The transcription level of *INO* in *Ar. thaliana* is higher at the early stages of seed development (Sun et al., 2021), and the expression level of *PgINO* was higher during the development of bisexual flowers in pomegranate. Therefore, *PgINO* was mainly involved in flower and seed development.

The ectopic expression analysis of *PgINO* revealed that *PgINO* overexpressing lines had 34.8 seeds per capsule, which was higher than that in WT. The number of seeds per capsule in *PgINO* complemented *ino* mutant lines was higher than that in WT and lower than that in *PgINO* overexpressed lines. This indicated that *PgINO* promoted seed numbers. *PgINO* was predominantly expressed in siliques of *PgINO* overexpressed lines, suggesting that *PgINO* was involved in regulating siliques and seed development. *VviINOs* are specifically expressed in grapevine flowers and young fruits (di Rienzo et al., 2021), which is consistent with our results of ectopic *PgINO* expression. This result revealed that *PgINO* regulated the development of siliques and seeds in pomegranates. The *V. vinifera INO* can successfully rescue the growth of the ovule outer integument and seed set in the Arabidopsis *ino* mutant (di Rienzo et al., 2021). In our study, the seed phenotype of *PgINO* complemented *ino* mutant lines was restored by *PgINO*, indicating that *PgINO* plays a crucial role in regulating ovule development.

INO has a conserved role in the growth of the outer integument of bitegmic ovules, and is essential for ovule development (Skinner et al., 2016). *INO* is a positive regulator of its expression, and *ANT* and *BEL1* act as direct or indirect regulators that help *INO* to establish its spatial expression pattern (Villanueva et al., 1999). *ANT* and *BEL1* are positive regulators of *INO* expression during ovule development (Balasubramanian and Schneitz, 2002), whereas *BEL1* has been suggested to be a negative regulator of *INO* in the chalaza (Villanueva et al., 1999). The protein interaction results demonstrated that PgBEL1 directly interacted with PgINO proteins, whereas that PgINO could not interact with MADS-box transcription factors to regulate ovule development in pomegranates. Our results revealed that PgINO directly regulated PgBEL1 expression, indicating a conservative regulatory relationship of this protein in pomegranate.

Analysis of regulatory relations among ovule identify genes

The analyses of ovule identify genes expression patterns in WT and transgenic Arabidopsis revealed that *PgCRC* and *PgINO* were highly expressed in siliques, and the expression of *PgSTK* was strongly detected in siliques and flowers. Previous studies have shown that *AP3*, *PI*, and *AG* combine with *SEP* to activate *CRC* expression in the nectary and carpel

(Lee et al., 2005). *AtSEP3* was highly expressed in young siliques of the *PgCRC* transgenic lines, suggesting that *PgCRC* activity could promote the expression of *AtSEP3* at the transcript level in young siliques. The expression analysis of *INO* and *STK* indicated that the regulation of *STK* by *INO* was involved in inflorescence and silique development at the transcriptional level. In Arabidopsis, *INO* is regulated by the upstream genes, *ANT* and *BEL1*, to regulate integument development (Balasubramanian and Schneitz, 2002; Simon et al., 2017). Moreover, the expression level of *AtBEL1* in young siliques of 35S::*PgINO* lines was higher than that of WT, but the expression pattern was opposite in mature siliques. *AtBEL1* transcriptional level of 35S::*PgCRC* transgenic lines was significantly lower than that in WT. Based on these results, we speculated that *BEL1* might be an upstream gene to regulate *CRC* and *INO* during flowers and siliques development.

PgBEL1 interacted with ovule identity proteins in the MADS-box family

The ABCDE models of flower development have been established for several genes encoding MADS-box transcription factors (Acri-Nunes-Miranda and Mondragón-Palomino, 2014; Theißen et al., 2016; Li et al., 2019). The C-function MADS-box genes including *AG*, *SHP1* and *SHP2* have functional redundancies in the development of female reproductive organs and fruits (Pinyopich et al., 2003; Brambilla et al., 2007; Zhao et al. 2021). *STK* (*AGL11*) is the only D-function gene in the MADS-box gene family, and *STK*, *SHP1*, and *SHP2* redundantly control ovule identity (Favaro et al. 2003; Pinyopich et al. 2003). Previous studies have indicated that the MADS-box ovule identity factors interact with BEL1 to control integument identity and formation (Brambilla et al., 2007). Our previous results suggested that *PgBEL1* was involved in pomegranate bisexual flowers and pistil development (Zhao et al., 2021). Furthermore, our assays confirmed that PgBEL1 did not directly interact with PgAG and PgSTK, which is consistent with the results of previous studies (Brambilla et al., 2007). However, PgBEL1 directly interacted with PgSEP, suggesting that it acts as a molecular bridge linking PgBEL1 and MADS-box transcription factors (Wang et al., 2021b).

Floral development requires the unique interaction of E-function proteins with various floral organ-determining proteins (Kramer and Hall, 2005). In Arabidopsis, ovule identity is determined by a multimeric complex composed of E-class SEP proteins and AGAMOUS-like proteins (AG, SHP1, SHP2, and STK; Favaro et al., 2003). SEP can bridge interactions among STK, SHP1, SHP2, and BEL1, which together regulate ovule identity (Pinyopich et al., 2003; Matias-Hernandez et al., 2010; Mendes et al., 2013). Arabidopsis has four largely redundant genes in the *SEP* subfamily (*SEP1*, *SEP2*, *SEP3*, and *SEP4*) that interact with AG. This can be explained by the redundancy of SEP proteins as AG interactors (Pelaz et al., 2000; Ditta et al., 2004). In our

previous study, we identified four members of the SEP subfamily: PgSEP1, PgSEP3a, PgSEP3b, and PgSEP4 (Zhao et al., 2020b), which had a nuclear localization signal (Supplemental Figure 2). Phylogenetic analyses clearly placed PgSEP1, PgSEP3, and PgSEP4 within three distinct clades, and our results were identical to those of previous studies (Supplemental Figure 3; Soza et al., 2016). In Woad (*Isatis indigotica*), SEP4 interacts with other MADS proteins to determine the identity of the floral organ (Pu et al., 2020). The results of Y2H assays proved that PgSEP1/4 could interact with the PgAG and PgSTK proteins, suggesting that PgSEP proteins, in combination with other transcriptional factors, play a conserved role in specifying the identities of ovules (Wang et al., 2021b). During carpel development in Arabidopsis, the predicted AG-SEP complex may establish a positive-feedback loop, thus reinforcing CRC expression (Gómez-Mena et al., 2005). In this study, we identified the PgAG-PgSEP, PgSEP-PgBEL1, and PgBEL1-PgCRC dimers in pomegranates.

A model for ovule development and seed determination in pomegranate

Our experimental data showed that the ovule identity proteins PgBEL1, PgINO, and PgCRC are all involved in ovule development and seed determination in pomegranate. SEPs have been suggested to interact with CRC proteins (Lee et al., 2005); however, the YABBY transcription factors PgINO and PgCRC did not directly interact with MADS-box factors at the protein level in pomegranates. *PgBEL1*, *PgCRC*, and *PgINO* were expressed in the pistil, indicating that the PgBEL1-PgINO and PgBEL1-PgCRC dimers were involved in the regulation of ovule initiation and development. PgAG, PgBEL1, and PgWUS coordinated to regulate floral meristem and ovule development. Previous genetic and biochemical studies have demonstrated that BEL1 interacts with the AG-SEP dimer to regulate integument growth and activate downstream genes such as *INO* (Schneitz et al. 1997). We suspected that PgBEL1 proteins acted as molecular bridges, allowing the combination of MADS-domain and PgCRC/PgINO proteins to form higher order complexes that regulated ovule and seed development in pomegranates. Furthermore, PgBEL1 interacted with PgAG and PgSTK when they were present as dimers with PgSEP proteins. We speculated that the establishment of a regulatory pathway between CRC, INO, BEL1, and MADS-box proteins might have facilitated the promotion of ovule and seed development. Based on this hypothesis, we proposed a model for ovule development and seed determination in pomegranates (Figure 13).

Materials and methods

Plant material and growth conditions
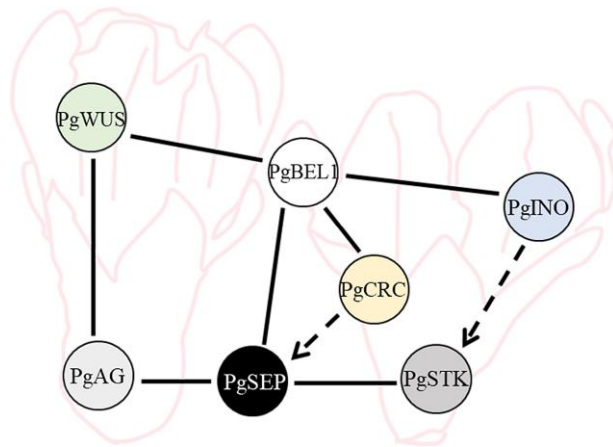From April to June in 2018–2020, we collected bisexual and functional male flowers from 6-year-old "Taishanhong"

Figure 13 A model for ovule development and seed determination in pomegranate. In flowers, PgAG and PgWUS synergistically regulate inflorescence meristem development. PgBEL1 acts as a molecular bridge linking PgCRC, PgINO, and MADS-box transcription factors to regulate ovule and seed development. There is no direct protein interaction between PgCRC, PgINO, and PgSTK/PgSEP; however, CRC and INO promoted the expression of *STK* and *SEP* during silique development in transgenic Arabidopsis. The solid lines indicate the confirmed interaction relationships, and the dashed lines represented regulatory relationships at the transcriptional level.

pomegranate (*P. granatum*) trees grown in the Baima Base for Teaching and Scientific Research of Nanjing Forestry University. The pomegranate trees were managed using conventional methods. Bisexual and functional male flowers were separated based on the bud vertical diameter (Chen et al., 2017a), which was expressed in a shortened style in functional male flowers (Wetzstein et al., 2011).

We used Arabidopsis (*Ar. thaliana*) from AraShare (https://www.arashare.cn/index/) as a transgenic material. The plants used in this study included the *ino* mutant, the *crc* mutant, and WT. The plants were grown in a 2:6:1 mixture of peat substrate: vermiculite: perlite under a 16 h light/8 h dark photoperiod at 22–24°C. Surface-sterilized transformant seeds were germinated on half-strength MS basal medium with 50 mg/L kanamycin. Plates were kept at 4°C for 2 days and then transferred to a growth chamber with a 16 h light/8 h dark photoperiod at 22–24°C. These conditions were used because *N. benthamiana* is known to grow under a 16 h light/8 h dark photoperiod at 22–24°C.

RNA extraction and gene cloning
Total RNA was isolated from developing floral buds using a plant total RNA extraction kit (BioTeke, Beijing, China). cDNA was prepared using a reverse transcription kit (PrimeScript™RT reagent kit with gDNA Eraser; TaKaRa, Beijing, China). CDSs of *PgCRC*, *PgINO*, and *PgBEL1* were cloned by homologous cloning (Supplemental Figure 4). Gene cloning primers were listed in Supplemental Table 3.

To obtain the ovule-related genes expression trends, the transcription levels of genes were obtained from pomegranate bisexual and functional male flowers transcriptome data (PRJNA754480) with vertical diameters of 5.0–10.0 mm (the first stage), 10.1–13.0 mm (the second stage), and 13.1–18.0 mm (the third stage; Zhao et al., 2022). RNA-seq and bioinformatics analyses were conducted by Novogene Company (Beijing, China). Sequencing libraries were generated using NEBNext® UltraTM RNA Library Prep Kit for Illumina® (NEB, USA). Index of pomegranate reference genome (ASM220158v1) was built using Hisat2 v2.0.5, clean reads were aligned to pomegranate genome using Hisat2 v2.0.5. FeatureCounts v1.5.0-p3 was used to count the reads numbers mapped to each gene. Then, FPKM was used to estimate gene expression levels using featureCounts (part of the Subread software). Twelve flower development genes were selected for RT-qPCR assays to confirm the reliability of the expression levels obtained from the RNA-Seq (Supplemental Figure 5). The heatmap of ovule-related genes was constructed with $\log_2$(FPKM) values using an online software (http://www.heatmapper.ca/expression/).

Plasmid construction and plant transformation
The 35S::PgCRC::GUS and 35S::PgINO::GUS constructs were generated using one-step cloning technology (Vazyme). The *PgCRC*, *PgBEL1*, and *PgINO* genes were cloned from flower cDNA using primers containing *Bam*HI and *Xba*I restriction sites (*Bam*HI: GATCC; *Xba*I: CTAGA), and the fragments were cloned into the pBI121 expression vector. The PgCRC::GFP and PgINO::GFP plasmids were similarly constructed and cloned into pBI121. The primers used for homologous recombination are listed in Supplemental Table 3. The vectors were constructed according to Prigge et al. (2005) and Chen et al. (2021).

To identify the functions of *PgCRC* and *PgINO*, WT plants were transformed by the floral dip method using *Ag. tumefaciens* strain GV3101. To assess whether *PgCRC* and *PgINO* could complement the *ino* and *crc* phenotypes, respectively, we transferred the 35S::PgCRC and 35S::PgINO constructs into *ino* and *crc* mutants. The transgenic lines were confirmed by PCR using primers to amplify the desired DNA fragments, and the *ino* and *crc* homozygous backgrounds were selected for genotyping by PCR amplification (Supplemental Table 3 and Figure 6 and 7).

Gene expression analysis with RT-qPCR
RT-qPCR was performed using an Applied Biosystems 7500 Real-Time PCR System (Applied Biosystems, MA, USA). The *PgActin* gene of pomegranate was used as the reference gene. All gene-specific primers were designed using Oligo 7 (Supplemental Table 3). The PCR program consisted of an initial denaturation at 95°C for 30 s, 40 cycles of 95°C for 5 s and 60°C for 34 s, followed by melt-curve analysis at 95°C for 15 s, 60°C for 60 s, and 95°C for 15 s. Three technical replicates were used for each reaction, and relative gene expression was determined using the $\Delta\Delta$CT method.

Subcellular localization

PgINO, *PgCRC* were cloned as *Bam*HI/*Xba*I fragments (for primer sequences see Supplemental Table 3) into the C-terminal GFP fusion vector containing the *35S* promoter. Positive clones of the GFP vector were screened by PCR, and positive *Agrobacterium* were activated to a D_{600} of 0.6–0.8 and then soaked in the six-leaf *N. benthamiana*. After 48 h, GFP expression was observed using a laser scanning confocal microscope (Carl Zeiss LSM710, the maximum spectral resolution is 3 mm, and the scanning parameters were set to automatic). The excitation wavelength of the GFP was 488 nm. The vector was constructed referring to the method of Zhang et al. (2018).

35S::PgSEP1::GFP, 35S::PgSEP3a::GFP, 35S::PgSEP3b::GFP, 35S::PgSEP4::GFP, 35S::PgAG::GFP and 35S::PgSTK::GFP were constructed in the same way, the primers were listed in Supplemental Table 4.

Observation of ovule development in pomegranate flowers

Paraffin slices were prepared using tissues from two types of pomegranate flowers (bisexual and functional male flowers). The flowers were classified according to their vertical diameter as follows: 3.0–5.0, 5.1–8.0, 8.1–10.0, 10.1–13.0, and 13.1–15.0 mm (Chen et al., 2017a; Zhao et al., 2020a). The samples were fixed in FAA solution, dehydrated with different concentrations of ethanol, and placed in a mixture of n-butanol and ethanol. Dehydration and transparency were performed according to previously published methods (Liang et al., 2020). The samples were embedded in paraffin wax, sectioned, and observed for the ovule development of pomegranates.

β-Glucuronidase staining

Histochemical staining was conducted to confirm the expression of the GUS reporter co-transformed with PgINO and PgCRC. For GUS staining, we collected whole inflorescences, capsules, and leaves, and incubated them in GUS staining solution with 2 mM X-Gluc overnight at 37°C. The tissues were subsequently decolored in 70% (v/v) ethanol, observed under a microscope, and photographed with a microscope camera (C3CMOS05100KPA (USB 2.0)).

Yeast two-hybrid assays

The full-length coding sequences (CDSs) of *PgCRC*, *PgINO*, *PgBEL1*, and MADS-box genes (Supplemental Figure 8) were independently cloned into the Y2H vectors, pGADT7 and pGBKT7, using suitable restriction sites (*Nde*I and *Bam*HI). All constructs were sequenced to confirm the gene sequences, and then transferred to the AH109 yeast strain (Wang et al., 2021a, 2021b). Clones carrying the desired DNA fragment were screened for auto-activation on SD medium, and protein–protein interactions were detected on SD medium lacking Trp, Leu, His, and Met. The combination of pGADT7 and pGBKT7 was used as a positive control, and the

X-α-Gal medium was used to detect colonies with positive hybridization. The primers used for vector construction are listed in Supplemental Tables 3 and 4.

Bimolecular fluorescence complementation assays

The BiFC assay was used to investigate the interactions between different proteins according to previously published methods (Wang et al., 2021a). Full-length sequences (without the stop codon) of *PgINO*, *PgCRC*, *PgBEL1*, *PgWUS*, and MADS-box genes were inserted into 35S-pSPYNE-YFP (N) and 35S-pSPYCE-YFP (C) vectors (restriction sites: *Bam*HI and *Sal*I; Wang et al., 2017). The primers used for vector construction are listed in Supplemental Tables 3 and 4. All constructs were transferred into GV3101 *Ag. tumefaciens*, and the cultures were adjusted to an OD_{600} of 0.8–1.0 using an infiltration buffer (10 mM $MgCl_2$ and 150 mM acetosyringone; pH 5.6). A 1:1 mixture of *Ag. tumefaciens* containing Vectors C and N was infiltrated into the leaves of *N. benthamiana*. The *N. benthamiana* plants were then cultivated in a growth chamber for 48 h and then used for the detection of double fluorescence signals. The assays were performed as previously described (Wang et al., 2017) with slight modification. Data from at least three independent experiments were used to confirm substantial regulatory effects.

Quantification and statistical analysis

The experimental data in this study represent at least three independent biological replicates. There were three replicates for the gene expression data and more than five replicates for counting the seed number. Data were analyzed using the SPSS software (22.0, USA).

Accession numbers

Sequence data from this article can be found in the GenBank/EMBL data libraries under accession numbers: OP828670 (*PgINO*), OP828671 (*PgCRC*), OP828678 (*PgBEL1*), OP828676 (*PgAG*), OP828677 (*PgSTK*), OP828672 (*PgSEP1*), OP828673 (*PgSEP3a*), OP828674 (*PgSEP3b*), OP828675 (*PgSEP4*), and OP828679 (*PgWUS*).

Supplemental data

The following materials are available in the online version of this article.

Supplemental Table S1. INO putatively orthologous proteins used for phylogenetic tree construction.

Supplemental Table S2. CRC putatively orthologous proteins used for phylogenetic tree construction.

Supplemental Table S3. Primers of PgINO, PgCRC, and PgBEL1 for gene cloning, subcellular localization, BiFC, Y2H, and RT-qPCR.

Supplemental Table S4. Primers of MADS-box genes for subcellular localization, BiFC, and Y2H.

Supplemental Figure S1. The control of BiFC.

Acknowledgments

Funding

References

Acri-Nunes-Miranda R, Mondragón-Palomino M (2014) Expression of paralogous *SEP-, FUL-, AG-* and *STK*-like MADS-box genes in wild-type and peloric *Phalaenopsis* flowers. Front Plant Sci **5**: 76

Alvarez J, Smyth DR (1999) *CRABS CLAW* and *SPATULA*, two *Arabidopsis* genes that control carpel development in parallel with *AGAMOUS*. Development **126**(11): 2377–2386

Alvarez J, Smyth DR (2002) CRABS CLAW and SPATULA genes regulate growth and pattern formation during gynoecium development in *Arabidopsis thaliana*. Int J Plant Sci **163**(1): 17–41

Baker SC, Robinson-Beers K, Villanueva JM, Gaiser JC, Gasser CS (1997) Interactions among genes regulating ovule development in *Arabidopsis thaliana*. Genetics **145**(4): 1109–1124

Balasubramanian S, Schneitz K (2002) NOZZLE Links proximal-distal and adaxial-abaxial pattern formation during ovule development in *Arabidopsis thaliana*. Development **129**(18): 4291–4300

Battaglia R, Colombo M, Kater MM (2009) The ins and outs of ovule development. Fruit development and seed dispersal. Annu Plant Rev **38**: 70–106

Baum SF, Eshed Y, Bowman JL (2001) The *Arabidopsis* nectary is an ABC-independent floral structure. Development **128**(22): 4657–4667

Bowman JL, Smyth DR (1999) CRABS CLAW, a gene that regulates carpel and nectary development in *Arabidopsis*, encodes a novel protein with zinc finger and helix-loop-helix domains. Development **126**(11): 2387–2396

Brambilla V, Battaglia R, Colombo M, Masiero S, Bencivenga S, Kater MM, Colombo L (2007) Genetic and molecular interactions between BELL1 and MADS-box factors support ovule development in *Arabidopsis*. Plant Cell **19**(8): 2544–2556

Cai YL, Lu XG, Zhu LW (1993a) Preliminary research on flower bud differentiation of pink pomegranate. Acta Hortic Sin **20**: 23–26 (in Chinese)

Cai YL, Wang DX, Zhu XT (1993b) Differentiation, development and structure of pomegranate pistil. J Anhui Agric Uni **20**(4): 349–352

Castañeda L, Giménez E, Pineda B, García-Sogo B, Ortiz-Atienza A, Micol-Ponce R, Angosto T, Capel J, Moreno V, Yuste-Lisbona FJ, et al. (2022) Tomato *CRABS CLAW* paralogues interact with chromatin remodelling factors to mediate carpel development and floral determinacy. New Phytologist **234**(3): 1059–1074

Chen LN, Zhang J, Li HX, Niu J, Xue H, Liu BB, Wang Q, Luo X, Zhang FH, Zhao DG, et al. (2017a) Transcriptomic analysis reveals candidate genes for female sterility in pomegranate flowers. Front Plant Sci **8**: 1430

Chen LN, Zhang J, Niu J, Li HX, Xue H, Liu BB, Xia XC, Zhang FH, Zhao DG, Cao SY (2017b) Cloning and functional verification of gene *PgAGL11* associated with the development of flower organs in pomegranate plant. Acta Hortic Sin **44**: 2089–2098

Chen YY, Hsiao YY, Li CI, Yeh CM, Mitsuda N, Yang HX, Chiu CC, Chang SB, Liu ZJ, Tsai WC (2021) The ancestral duplicated DL/CRC orthologs, PeDL1 and PeDL2, function in orchid reproductive organ innovation. J Exp Bot **8**(15): 195

di Rienzo V, Imanifard Z, Mascio I, Gasser CS, Skinner DJ, Pierri CL, Marini M, Fanelli V, Sabetta W, Montemurro C, et al. (2021) Functional conservation of the grapevine candidate gene *INNER NO OUTER* for ovule development and seed formation. Hortic Res **8**(1): 29

Ditta G, Pinyopich A, Robles P, Pelaz S, Yanofsky MF (2004) The *SEP4* gene of *Arabidopsis thaliana* functions in floral organ and meristem identity. Curr Biol **14**(21): 1935–1940

Favaro R, Pinyopich A, Battaglia R, Kooiker M, Borghi L, Ditta G, Yanofsky MF, Kater MM, Colombo L (2003) MADS-box protein complexes control carpel and ovule development in *Arabidopsis*. Plant Cell **15**(11): 2603–2611

Fourquin C, Primo A, Martínez-Fernández I, Huet-Trujillo E, Ferrándiz C (2014) The CRC orthologue from *Pisum sativum* shows conserved functions in carpel morphogenesis and vascular development. Ann Bot **114**: 1535–1544

Fourquin C, Vinauger-Douard M, Chambrier P, Berne-Dedieu A, Scutt CP (2007) Functional conservation between *CRABS CLAW* orthologues from widely diverged angiosperms. Ann Bot **100**(3): 651–657

Gallagher TL, Gasser CS (2008) Independence and interaction of regions of the INNER NO OUTER protein in growth control during ovule development. Plant Physiol **147**(1): 306–315

Gasser CS, Skinner DJ (2019) Development and evolution of the unique ovules of flowering plants. Curr Topics Dev Biol **131**: 373–399

Gómez-Mena C, de Folter S, Costa MMR, Angenent GC, Sablowski R (2005) Transcriptional program controlled by the floral homeotic gene *AGAMOUS* during early organogenesis. Development **132**(3): 429–438

Gong PC, Song CJ, Liu HY, Li PG, Zhang MS, Zhang JS, Zhang SH, He CY (2021) *Physalis floridana CRABS CLAW* mediates neofunctionalization of *GLOBOSA* genes in carpel development. J Exp Bot **72**(20): 6882–6903

Gross T, Broholm S, Becker A (2018) CRABS CLAW acts as a bifunctional transcription factor in flower development. Front Plant Sci **9**: 835

Immink RGH, Tonaco IAN, de Folter S, Shchennikova A, van Dijk ADJ, Busscher-Lange J, Borst JW, Angenent GC (2009) SEPALLATA3: the 'glue' for MADS box transcription factor complex formation. Genome Biol **10**(2): R24

Kelley DR, Arreola A, Gallagher TL, Gasser CS (2012) ETTIN (ARF3) physically interacts with KANADI proteins to form a functional complex essential for integument development and polarity determination in *Arabidopsis*. Development **139**(6): 1105–1109

Kramer EM, Hall JC (2005) Evolutionary dynamics of genes controlling floral development. Curr Opin Plant Biol **8**(1): 13–18

Lee JY, Baum SF, Alvarez J, Patel A, Chitwood DH, Bowman JL (2005) Activation of *CRABS CLAW* in the nectaries and carpels of *Arabidopsis*. Plant Cell **17**(1): 25–36

Li S, Chen KS, Grierson D (2019) A critical evaluation of the role of ethylene and MADS transcription factors in the network controlling fleshy fruit ripening. New Phytol **221**(1): 1724–1741

Liang JJ, Guan PY, Liu ZH, Wang Y, Xing JY, Hu JF (2020) The *VvSUPERMAN-like* gene is differentially expressed between bicarpellate and tricarpellate florets of *Vitis vinifera* L. Cv. 'Xiangfei' and its heterologous expression reduces carpel number in tomato. Plant Cell Physiol **61**(10): 1760–1774

Lora J, Hormaza JI, Herrero M (2015) Transition from two to one integument in Prunus species: expression pattern of *INNER NO OUTER* (INO), *ABERRANT TESTA SHAPE* (ATS) and *ETTIN* (ETT). New Phytol **208**(2): 584–595

Matias-Hernandez L, Battaglia R, Galbiati F, Rubes M, Eichenberger C, Grossniklaus U, Kater MM, Colombo L (2010) *VERDANDI* Is a direct target of the MADS domain ovule identity complex and affects embryo sac differentiation in *Arabidopsis*. Plant Cell **22**(6): 1702–1715

McAbee JM, Hill TA, Skinner DJ, Izhaki A, Hauser BA, Meister RJ, Venugopala Reddy G, Meyerowitz EM, Bowman JL, Gasser CS (2006) *ABERRANT TESTA SHAPE* encodes a KANADI family member, linking polarity determination to separation and growth of *Arabidopsis* ovule integuments. Plant J **46**(3): 522–531

Meister RJ, Kotow LM, Gasser CS (2002) SUPERMAN Attenuates positive *INNER NO OUTER* autoregulation to maintain polar development of *Arabidopsis* ovule outer integuments. Development **129**(18): 4281–4289

Mendes MA, Guerra RF, Berns MC, Manzo C, Masiero S, Finzi L, Kater MM, Colombo L (2013) MADS Domain transcription factors mediate short-range DNA looping that is essential for target gene expression in *Arabidopsis*. Plant Cell **25**(7): 2560–2572

Ming F, Ma H (2009) A terminator of floral stem cells. Genes Devel **23**: 1705–1708

Morel P, Heijmans K, Ament K, Chopy M, Trehin C, Chambrier P, Rodrigues Bento SR, Bimbo A, Vandenbussche M (2018) The foral C-lineage genes trigger nectary development in *Petunia* and *Arabidopsis*. Plant Cell **30**(9): 2020–2037

Ó'Maoiléidigh DS, Wuest SE, Rae L, Raganelli A, Ryan PT, Kwasniewska K, Das P, Lohan AJ, Loftus B, Graciet E, et al. (2013) Control of reproductive floral organ identity specification in *Arabidopsis* by the C function regulator AGAMOUS. Plant Cell **25**(7): 2482–2503

Orashakova S, Lange M, Lange S, Wege S, Becker A (2009) The *CRABS CLAW* ortholog from California poppy (*Eschscholzia californica*, Papaveraceae), *EcCRC*, is involved in floral meristem termination, gynoecium differentiation and ovule initiation. Plant J **58**(4): 682–693

Pelaz S, Ditta GS, Baumann E, Wisman E, Yanofsky MF (2000) B and C floral organ identity functions require SEPALLATA MADS-box genes. Nature **405**(6782): 200–203

Phukela B, Geeta R, Das S, Tandon R (2020) Ancestral segmental duplication in Solanaceae is responsible for the origin of *CRCa-CRCb* paralogues in the family. Mol Genet Genom **295**(3): 563–577

Pinyopich A, Ditta GS, Savidge B, Liljegren SJ, Baumann E, Wisman E, Yanofsky MF (2003) Assessing the redundancy of MADS-box genes during carpel and ovule development. Nature **424**(6944): 85–88

Prigge MJ, Otsuga D, Alonso JM, Ecker JR, Drews GN, Clark SE (2005) Class III homeodomain-leucine zipper gene family members have overlapping, antagonistic, and distinct roles in Arabidopsis development. Plant Cell **17**(1): 61–76

Pu ZQ, Ma YY, Lu MX, Ma YQ, Xu ZQ (2020) Cloning of a *SEPALLATA4*-like gene (*IiSEP4*) in *Isatis indigotica* fortune and characterization of its function in *Arabidopsis thaliana*. Plant Physiol Biochem **154**: 229–237

Reiser L, Modrusan Z, Margossian L, Samach A, Ohad N, Haughn GW, Fischer RL (1995) The BELL1 gene encodes a homeodomain protein involved in pattern formation in the *Arabidopsis* ovule primordium. Cell **83**(5): 735–742

Robinson-Beers K, Pruitt RE, Gasser CS (1992) Ovule development in wild-type Arabidopsis and two female-sterile mutants. Plant Cell **4**(10): 1237–1249

Sablowski R (2015) Control of patterning, growth, and differentiation by floral organ identity genes. J Exp Bot **66**(4): 1065–1073

Schneitz K, Hülskamp M, Kopczak SD, Pruitt RE (1997) Dissection of sexual organ ontogenesis: a genetic analysis of ovule development in *Arabidopsis thaliana*. Development **124**(7): 1367–1376

Schneitz K, Hülskamp M, Pruitt RE (1995) Wild-type ovule development in *Arabidopsis thaliana*: a light microscope study of cleared whole-mount tissue. Plant J **7**(5): 731–749

Siegfried KR, Eshed Y, Baum SF, Otsuga D, Drews GN, Bowman JL (1999) Members of the YABBY gene family specify abaxial cell fate in *Arabidopsis*. Development **126**(18): 4117–4128

Simon MK, Skinner DJ, Gallagher TL, Gasser CS (2017) Integument development in Arabidopsis depends on interaction of YABBY protein INNER NO OUTER with coactivators and corepressors. Genetics **207**(4): 1489–1500

Skinner DJ, Brown RH, Kuzoff RK, Gasser CS (2016) Conservation of the role of INNER NO OUTER in development of unitegmic ovules of the Solanaceae despite a divergence in protein function. BMC Plant Biol **16**(1): 143

Soza VL, Snelson CD, Hazelton KD, Di Stilio VS (2016) Partial redundancy and functional specialization of E-class *SEPALLAT* genes in an early-diverging eudicot. Dev Biol **419**(1): 143–155

Sun L, Wei YQ, Wu KH, Yan JY, Xu JN, Wu YR, Li GX, Xu JM, Harberd NP, Ding ZJ, et al. (2021) Restriction of iron loading into developing seeds by a YABBY transcription factor safeguards successful reproduction in *Arabidopsis*. Mol Plant **14**(10): 1624–1639

Theißen G, Melzer R, Rümpler F (2016) MADS-domain transcription factors and the floral quartet model of flower development: linking plant development and evolution. Development **143**(18): 3259–3271

Vandenbussche M, Zethof J, Souer E, Koes R, Tornielli GB, Pezzotti M, Ferrario S, Angenent GC, Gerats T (2003) Toward the analysis of the petunia MADS box gene family by reverse and forward transposon insertion mutagenesis approaches: b, C, and D floral organ identity functions require *SEPALLATA*-like MADS box genes in petunia. Plant Cell **15**(11): 2680–2693

Villanueva JM, Broadhvest J, Hauser BA, Meister RJ, Schneitz K, Gasser CS (1999) *INNER NO OUTER* regulates abaxial-adaxial patterning in *Arabidopsis* ovules. Genes and Development **13**(23): 3160–3169

Wang N, Xu HF, Jiang SH, Zhang ZY, Lu NL, Qiu HR, Qu CZ, Wang YC, Wu SJ, Chen XS (2017) MYB12 And MYB22 play essential roles in proanthocyanidin and flavonol synthesis in red-fleshed apple (*Malus sieversii* f. *niedzwetzkyana*). Plant J **90**(2): 276–292

Wang YC, Mao ZL, Jiang HY, Zhang ZY, Wang N, Chen XS (2021a) Brassinolide inhibits flavonoid biosynthesis and red-flesh coloration via the MdBEH2.2–MdMYB60 complex in apple. J Exp Bot **72**(18): 6382–6399

Wang Y, Liu ZH, Wu J, Hong L, Liang JJ, Ren YM, Guan PY, Hu JF (2021b) MADS-box protein complex VvAG2, VvSEP3 and VvAGL11 regulates the formation of ovules in *Vitis vinifera* L. cv. 'Xiangfei'. Genes (Basel) **12**(5): 647

Western TL, Haughn GW (1999) BELL1 and AGAMOUS genes promote ovule identity in *Arabidopsis thaliana*. Plant J **18**(3): 329–336

Wetzstein HY, Ravid N, Wilkins E, Martinelli AP (2011) A morphological and histological characterization of bisexual and male flower types in pomegranate. J Am Soc Hortic Sci **136**(2): 83–92

Wetzstein HY, Yi WG, Porter JA, Ravid N (2013) Flower position and size impact ovule number per flower, fruitset, and fruit size in pomegranate. J Am Soc Hortic Sci **138**(3): 159–166

Xu G, Huang J, Lei SK, Sun XG, Li X (2019) Comparative gene expression profile analysis of ovules provides insights into *Jatropha curcas* L. Ovule development. Sci Rep **9**(1): 15973

Zhang CL, Wei LD, Wang WJ, Qi WQ, Cao Z, Li H, Bao MZ, He YH (2020) Identification, characterization and functional analysis of *AGAMOUS* subfamily genes associated with floral organs and seed development in marigold (*Tagetes erecta*). BMC Plant Biol **20**(1): 439

Zhang HY, Yu PL, Zhao JH, Jiang HL, Wang HY, Zhu YF, Botella MA, Samaj J, Li CY, Lin JX (2018) Expression of tomato prosystemin gene in *Arabidopsis* reveals systemic translocation of its mRNA and confers necrotrophic fungal resistance. New Phytologist **217**(2): 799–812

Zhao YJ, Liu CY, Ge DP, Yan M, Ren Y, Huang XB, Yuan ZH (2020a) Genome-wide identification and expression of YABBY genes family during flower development in *Punica granatum* L. Gene **752**: 144784

Zhao YJ, Liu CY, Zhao XQ, Wang YY, Yan M, Yuan ZH (2021) Cloning and spatiotemporal expression analysis of *PgWUS* and *PgBEL1* in *Punica granatum*. Acta Hortic Sin **48**: 355–366 (in Chinese)

Zhao YJ, Wang YY, Zhao XQ, Yan M, Ren Y, Yuan ZH (2022) *ARF6s* Identification and function analysis provide insights into flower development of *Punica granatum* L. Front Plant Sci **13**: 833747

Zhao YJ, Zhao HL, Wang YY, Zhang XH, Zhao XQ, Yuan ZH (2020b) Genome-wide identification and expression analysis of MIKC-type MADS-box gene family in *Punica granatum* L. Agronomy **10**(8): 1197